resolution inherent in X-ray crystallographic data collection, another low-occupancy conformation of Glu-270 and/or the zinc-bound water, or BMBP itself, may effect the kinetically slow exchange, resulting in a time-averaged structure showing little or no sign of such an alternate conformation.

**Acknowledgment.** We thank the National Institutes of Health for Grant GM 06920 in support of this research and the National Science Foundation for Grant PCM-77-11398 for support of the computational facility. We thank Patricia Christianson for her help with the figures, the Jane Coffin Childs Memorial Fund for Medical Research for a postdoctoral fellowship to L.C.K., and AT&T Bell Laboratories for a doctoral fellowship to D.W.C.

## A Quantitative Theory of Mass Spectral Fragmentation Patterns

J. Silberstein and R. D. Levine*

*The Fritz Haber Research Center for Molecular Dynamics, The Hebrew University Jerusalem 91904, Israel*

*Received July 30, 1985*

The discovery of laser-pumped multiphoton ionization–fragmentation[1,2] led to renewed interest in the dissociation processes of energy-rich polyatomic ions. Often, the laser pulse is long enough in time to allow absorption of light by fragment ions.[1,3-5] A simpler process is thus fragmentation induced by electron impact where all the available energy is deposited in the parent molecular ion. Any theory of the fragmentation pattern should thus work for mass spectral patterns. Yet even on a qualitative level the observed mass spectrum for electron impact is different than the laser-induced one. The latter pattern can be varied, often from a very soft ionization producing mostly the parent to very extensive fragmentation, by increasing the laser power. In an attempt to interpret such observations, we have proposed[6] that the fragmentation pattern is governed primarily by the mean energy, $\langle E \rangle$, absorbed per parent molecule. This has indeed been verified.[7,8] Yet such an assumption (which is part also of the more detailed mechanistic approach[9]) leads to a very characteristic qualitative behavior of the predicted fragmentation pattern. At very low values of $\langle E \rangle$ (measured from the ground state of the parent ion), one obtains mostly the parent itself. As $\langle E \rangle$ is increased, the spectrum consists of primary dissociation products. At high $\langle E \rangle$ values the spectrum consists mostly of "energy expensive" products. Such multiphoton ionization fragmentation patterns where the parent as well as energy expensive ions are present is interpreted in the mechanistic approach[9] as due to selective absorption of energy by secondary ions. Indeed, for short laser pulses[10] the mass spectrum is "narrower". Electron impact fragmentation typically produces little of the energy expensive ions. Otherwise, however, it spans a wider mass range, showing simultaneously both low and intermediate energy product ions.

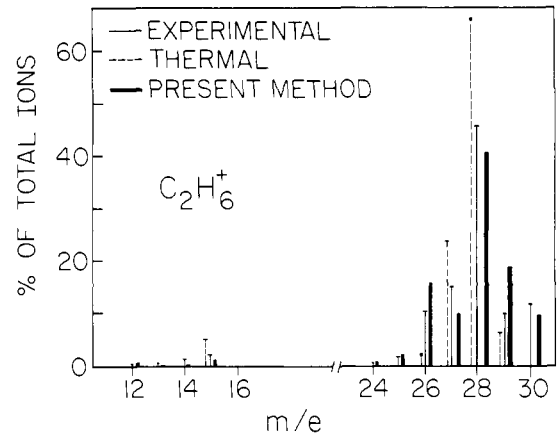


**Figure 1.** Measured[12] electron impact mass spectrum off ethane and two sets of computational results: (i) a computation based on specifying just the mean energy, $\langle E \rangle$, of excitation per parent molecule. This leads to a thermallike distribution $f(E)$ of the excitation energy. We have used that value of $\langle E \rangle$ that best fits the observed spectrum ($\langle E \rangle$ = 4.3 eV above the ground state of $C_2H_6^+$). (ii) Results obtained by using a wider distribution of energy with $\langle E \rangle$ = 5.7 eV.

The computational procedure[9] is to determine the branching fractions into all possible dissociation channels of the parent ion. This is done by seeking that set of branching fractions which is of maximal entropy subject to constraints. It is the constraints that specify the nature of the process. The simplest constraint and one that works well for laser-induced processes is to specify the mean energy, $\langle E \rangle$, absorbed per parent molecule. The final answer is then remarkably simple.[9] The branching fraction for any dissociation pathway of the parent ion is fully determined as a product of relevant partition functions. As a concrete example consider computing the fragmentation pattern of $C_2H_6^+$. The branching fraction for, say, the $C_2H_6^+ \rightarrow C_2H_4^+ + H_2$ reaction is given by

$$q = Q_{C_2H_4^+} Q_{H_2} Q_T / N \qquad (1)$$

$Q_X$ is the partition function for molecule X, here X is $C_2H_4^+$ or $H_2$ and $Q_T$ is the partition function for the relative translational motion of the fragments. $N$ is the normalization constant such that the sum of branching fractions for all possible dissociation processes is unity.

The fragmentation pattern can therefore be computed using standard thermochemical data of stable species[11] without adjustable parameters. The value of the temperature at which the partition functions are to be evaluated is that which reproduces the mean energy $\langle E \rangle$ per parent molecule. This approach works reasonably well for multiphoton excitation but fails, Figure 1, to provide a quanitative agreement for electron impact mass spectra. The primary deficiency, as seen in Figure 1 and in other cases as well, is that when $\langle E \rangle$ is chosen so as to provide the best possible fit to the observed spectrum, hardly any undissociated parent survives.

The maximum entropy formalism determines the energy distribution in the energy-rich parent ion from the given value of $\langle E \rangle$. We here consider the possibility that the resulting distribution for electron impact excitation is too narrow. To broaden the theoretical distribution one needs to specify additional moments of the distribution besides $\langle E \rangle$. Once that is done, the agreement with the electron impact fragmentation pattern[12] becomes quantitative, Figure 1.

The important practical point is that even when additional moments of the energy distribution are specified the branching fraction can still be computed from the densities of states of the

(1) Schlag, E. W.; Neusser, H. J. *Acc. Chem. Res.* **1983**, *16*, 355.
(2) Bernstein, R. B. *J. Phys. Chem.* **1982**, *86*, 1178.
(3) Durant, J. L.; Rider, D. M.; Anderson, S. L.; Proch, F. D.; Zare, R. N. *J. Chem. Phys.* **1984**, *80*, 1817.
(4) Koplitz, B. D.; McVey, J. K. J. *Chem. Phys.* **1984**, *80*, 2271.
(5) Stiller, S. W.; Johnston, M. V. *J. Phys. Chem.* **1985**, *89*, 2717.
(6) Silberstein, J.; Levine, R. D. *Chem. Phys. Lett.* **1980**, *74*, 6. Silberstein, J.; Levine, R. D. *J. Chem. Phys.* **1981**, *75*, 5735.
(7) Lichtin, D. A.; Bernstein, R. B.; Newton, K. R. *J. Chem. Phys.* **1981**, *75*, 5728.
(8) Lubman, D. M. *J. Phys. Chem.* **1981**, *85*, 3752.
(9) Silberstein, J.; Levine, R. D. *Chem. Phys. Lett.* **1983**, *99*, 1; *J. Phys. Chem.*, in press.
(10) Gobeli, D. A.; Simon, J. D.; El-Sayed, M. A. *J. Phys. Chem.* **1981**, *88*, 3949.
(11) Rosenstock, H. M.; Draxl, K.; Steiner, D. W.; Herron, J. T. *J. Phys. Chem. Ref. Data, Suppl.* **1977**, *6*, (1).
(12) Mass Spectral Data, American Petroleum Institute, Research Project 44, Carnegie Institute of Technology, Pittsburgh, PA, 1955.

0002-7863/85/1507-8283$01.50/0 

products that are available from thermochemical data alone. The details of the computational procedure will be given elsewhere, but the essence is as follows. Starting with a product of ordinary partition functions, as in (1), we use the steepest descent procedure[13] to determine the density of states $\rho(E)$ for the particular dissociation channel. Then a generalized partition function is computed as

$$Q = \int_0^\infty \rho(E) f(E)\, dE \qquad (2)$$

Here $f(E)$ is the energy deposition function. The branching fraction $q$ is given by $q = Q/N$. If $f(E) = \exp(-\beta E)$ then (2) leads back to (1). If we specify both $\langle E \rangle$ and, say, $\langle E^2 \rangle$ then $f(E) = \exp(-\beta E - \gamma E^2)$, where the value of $\gamma$ is such so as to reproduce the value of $\langle E^2 \rangle$, etc.

To achieve a distribution in energy that is *wider* than thermal we have used $f(E) = \exp(-\alpha E^{1/2} - \beta E - \gamma E^2)$, which is the distribution of maximal entropy subject to given values for $\langle E^{1/2} \rangle$, $\langle E \rangle$, and $\langle E^2 \rangle$. For the present results shown in Figure 1, $\langle E^{1/2} \rangle^2$, $\langle E \rangle$, and $\langle E^2 \rangle^{1/2}$ have the values 4.3, 5.7, and 8.5 eV, respectively. For the narrower, thermallike distribution the corresponding values are 4.12, 4.3, and 4.6 eV.

The computational results for $C_2H_6$ and other systems suggest that there are two primary reasons for the differences between the multiphoton ionization[1,2] and the electron impact mass spectrum: (i) Energy input into the secondary ions is absent in the latter.[9] That, however, can also be achieved in the former using short (picosecond) laser pulses. (ii) The energy distribution of the parent ion produced by electron impact is wider. That is consistent with the very wide energy distributions assumed in the QET-type computations[14] and indicated by threshold-law considerations.[15,16] The narrower laser-pumped distributions makes them more useful for analytical applications of mass spectrometry.

**Acknowledgment.** The Fritz Haber Research Center is supported by the Minerva Gesellschaft für die Forschung, mbH, München, BRD.

(13) Hoare, M. R. *J. Chem. Phys.* **1969**, *52*, 113; **1969**, *52*, 5695.
(14) Vestal, M. L. *J. Chem. Phys.* **1965**, *43*, 1356.
(15) Stockbauer, R.; Ingram, M. G. *J. Chem. Phys.* **1971**, *54*, 2242.
(16) Meisels, G. G.; Chen, C. T.; Giessner, B. G.; Emmel, R. H. *J. Chem. Phys.* **1972**, *56*, 793. Scheppele, S. E.; Mitchum, R. K.; Kinnerberg, K. F.; Meisels, G. G.; Emmel, R. H. *J. Am. Chem. Soc.* **1973**, *95*, 5105.

## Preparation and Structures of Novel Di- and Trinuclear Clusters of Iridium(II) without Carbonyl Ligands

F. Albert Cotton,* Pascual Lahuerta, Mercedes Sanau, and Willi Schwotzer

*Department of Chemistry and Laboratory for Molecular Structure and Bonding, Texas A&M University College Station, Texas 77843*

*Received August 19, 1985*

Despite rapid development of the chemistry of metal–metal-bonded complexes[1] there are still large untouched areas. One of these underinvestigated fields is that of iridium cluster compounds with ligands other than carbon monoxide.[2]

We wish to report here the synthesis and structure of an Ir(II) complex, $Ir_2(\mu^2\text{-}I)_2I_2(COD)_2$ (**1**) (COD = 1,5-cyclooctadiene)

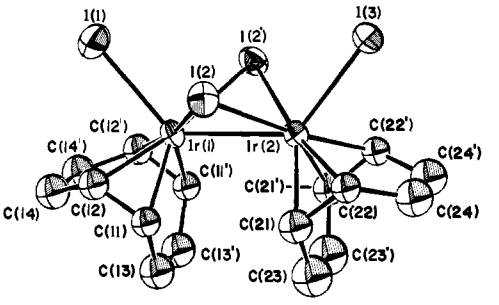


**Figure 1.** ORTEP view of $[Ir(COD)I_2]_2$. All atoms are represented by their ellipsoids of thermal vibration at the 40% probability level.

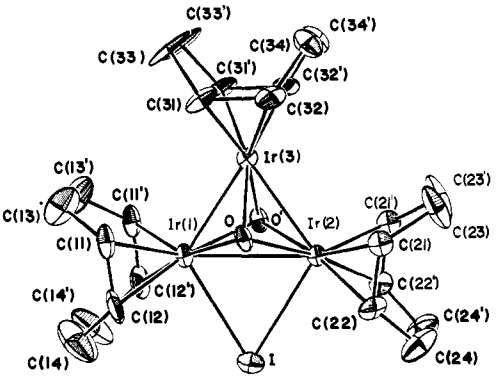


**Figure 2.** ORTEP view of $Ir_3(\mu^3\text{-}O)_2(\mu^2\text{-}I)(COD)_3$.

which we expect to be a starting material for the synthesis of cluster compounds. Reaction of **1** with silver acetate afforded, among other products, the trinuclear cluster $Ir_3(\mu^3\text{-}O)_2(\mu^2\text{-}I)(COD)_3$ (**2**). It is a bioxo-capped trimer of a configuration unprecedented among late transition metals.

Reaction of equimolar amounts of $Ir_2(OMe)_2(COD)_2$[3] and $I_2$ in $CH_2Cl_2$ for 30 min, followed by partial evaporation of the solvent and precipitation with hexane, afforded the dark red crystalline compound **1**. An ORTEP drawing is given in Figure 1.[4] The dimeric molecule has crystallographically imposed $C_{2v}$ symmetry and is composed of two square pyramids sharing an edge. The Ir–Ir distance is 2.914 (1) Å and indicative of bonding interaction between the two metal atoms. The fact that there is an 18-electron count for each metal center if an Ir–Ir bond is assumed supports this.

Reaction of **1** with $Ag(O_2CCH_3)$ in $CH_2Cl_2$ leads instantaneously to a voluminous precipitate of AgI. The reaction mixture, after filtration, was investigated by TLC. On silica gel we find that a large fraction of the product mixture is irreversibly adsorbed at the starting point. Of the moving zones the one corresponding to the trimeric cluster **2** is the most abundant fraction. It was isolated by column chromatography (silica gel, $CH_2Cl_2$) reproducibly in yields of ca. 5%. While we are not suggesting, in light of the low yield, that this is a good synthesis for **2**, we report it here because the cluster is a surprising molecule for Ir to form. The synthetic procedures are presently under revision. The cluster compound is depicted in Figure 2.[5] It consists of an isosceles triangle of Ir atoms, bicapped by $\mu^3$-O atoms and containing one $\mu^2$-I bridge. This leads to a square-prismatic coordination polyhedron for Ir1 and Ir2 whereas Ir3 exhibits a square-planar coordination geometry. The trimer is then composed of the three-coordination polyhedra sharing the O···O edge.

Bioxo-capped trinuclear clusters are unprecedented among the late transition metals but are an important structural type for

(1) Cotton, F. A.; Walton, R. A. "Multiple Bonds between Metal Atoms"; Wiley: New York, 1982.
(2) Recent reports on dimeric Ir(II) clusters. (a) Rasmussen, P. G.; Anderson, J. E.; Bailey, O. H.; Milton Tamres *J. Am. Chem. Soc.* **1985**, *107*, 279. (b) Beveridge, K. A.; Bushnell, G. W.; Dixon, K. R.; Eadie, D. T.; Stobart, S. R.; Atwood, J. L.; Zaworotko, M. J. *J. Am. Chem. Soc.* **1982**, *104*, 920. (c) Coleman, A. W.; Eadie, D. T.; Stobart, S. R.; Zaworotko, M. J.; Atwood, J. L. *J. Am. Chem. Soc.* **1982**, *104*, 922. (d) Kalk, P.; Bonnet, J. J. *Organometallics* **1982**, *1*, 1211. (e) Bonnet, J. J.; Thorez, A.; Maisonnat, A.; Poilblanc, R. *J. Am. Chem. Soc.* **1979**, *101*, 5940. (f) Angoleta, M.; Malatesta, L.; Caglio, G. J. *Chem. Soc., Dalton Trans.* **1977**, *2131*.
(3) Pannetier, G.; Fougeroux, P.; Bonnaire, R.; Platzer, N. *J. Less-Common Met.* **1971**, *24*, 83.
(4) Dark red crystals from $CH_2Cl_2$/hexane–acetone: orthorhombic *Pnma*: $a = 16.248$ (9) Å, $b = 10.827$ (10) Å, $c = 11.739$ (9) Å; $Z = 4$; $R = 0.032$, $R_w = 0.043$.
(5) Dark red crystals from $CH_2Cl_2$/hexane–acetone; monoclinic $C2/c$; $a = 22.205$ (3) Å, $b = 11.967$ (2) Å, $c = 19.042$ (4) Å; $\beta = 99.09$ (2)°; $Z = 8$; $R = 0.046$, $R_w = 0.063$.

0002-7863/85/1507-8284$01.50/0 